# High Affinity Binding of Hsp90 Is Triggered by Multiple Discrete Segments of Its Kinase Clients†

Bradley T. Scroggins, Thomas Prince, Jieya Shao, Sheri Uma, Wenjun Huang, Yanwen Guo, Bo-Geon Yun, Karla Hedman, Robert L. Matts,* and Steven D. Hartson

*Department of Biochemistry and Molecular Biology, Oklahoma State University, Stillwater, Oklahoma 74078-3035*

*Received June 12, 2003; Revised Manuscript Received August 29, 2003*

ABSTRACT: The 90 kDa heat shock protein (Hsp90) cooperates with its co-chaperone Cdc37 to provide obligatory support to numerous protein kinases involved in the regulation of cellular signal transduction pathways. In this report, crystal structures of protein kinases were used to guide the dissection of two kinases [the Src-family tyrosine kinase, Lck, and the heme-regulated eIF2α kinase (HRI)], and the association of Hsp90 and Cdc37 with these constructs was assessed. Hsp90 interacted with both the N-terminal (NL) and C-terminal (CL) lobes of the kinases' catalytic domains. In contrast, Cdc37 interacted only with the NL. The Hsp90 antagonist molybdate was necessary to stabilize the interactions between isolated subdomains and Hsp90 or Cdc37, but the presence of both lobes of the kinases' catalytic domain generated a stable salt-resistant chaperone−client heterocomplex. The Hsp90 co-chaperones FKBP52 and p23 interacted with the catalytic domain and the NL of Lck, whereas protein phosphatase 5 demonstrated unique modes of kinase binding. Cyp40 was a salt labile component of Hsp90 complexes formed with the full-length, catalytic domains, and N-terminal catalytic lobes of Lck and HRI. Additionally, dissections identify a specific kinase motif that triggers Hsp90's conformational switching to a high-affinity client binding state. Results indicate that the Hsp90 machine acts as a versatile chaperone that recognizes multiple regions of non-native proteins, while Cdc37 binds to a more specific kinase segment, and that concomitant recognition of multiple client segments is communicated to generate or stabilize high-affinity chaperone−client heterocomplexes.

In vivo, the 90 kDa heat shock protein (Hsp90)[1] function is essential for the biogenesis and support of numerous cellular proteins that control cell physiology (reviewed in refs *1*−*8*). However, Hsp90 does not appear to facilitate the biogenesis of all proteins; instead, Hsp90's clientele seems to be restricted to a diverse clientele of regulatory proteins (reviewed in refs *1*−*8*). Thus, Hsp90 has been dubbed the "signal transduction chaperone" (*3*, *4*, *9*−*11*) due to its specific action at critical interfaces between converging pathways of protein folding and regulation (*12*−*16*). Additionally, Hsp90 supports mutational drift (*17*, *18*) of signal transduction proteins (*12*, *16*, *19*, *20*), and this support may be essential to the microevolution of transformed cell populations (*7*). Thus, Hsp90's role as the signal transduction chaperone makes it an attractive target for efforts to manipulate the growth and differentiation of normal and aberrant cell populations (*7*, *8*). Pharmacological inhibition of Hsp90 is currently being pursued in clinical trials as a strategy to treat human cancers, and the ability of the Hsp90 inhibitor geldanamycin to modulate immune function has been investigated (*21*, *22*).

Despite over a decade of intense study, the basis for Hsp90's recognition of its diverse clients remains one of the primary puzzles in the field. The endoplasmic reticulum homologue of Hsp90, Grp94, specifically binds small peptides in vivo and facilitates the assembly of antigen presenting complexes (*23*−*27*). In vitro studies indicate that Hsp90, like Grp94, can interact with short peptides (*28*−*30*) that represent segments present on client proteins, and these peptides can disrupt interactions between Hsp90 and steroid receptor clients. Studies using site-directed and deletion mutagenesis (*31*−*37*) have identified potential sites within steroid hormone receptors and protein kinases that may be recognized by Hsp90, but no primary, secondary, and/or tertiary structural features that may be responsible for Hsp90-client recognition have yet to be clearly defined.

Key to Hsp90 function is its association with a coterie of nonclient co-chaperone partners, as well as Hsp90's own

† This work was supported by the National Institute of Health (National Institute of General Medicine GM51608 to R.L.M.), the American Heart Association (Award No.: 0250556N to R.L.M.), the Oklahoma Center for the Advancement of Science and Technology (HN6-018 to S.D.H.), and by the Oklahoma Agricultural Experiment Station (Project 1975).

* For correspondence: Robert L. Matts, 246 NRC, Department of Biochemistry and Molecular Biology, Oklahoma State University, Stillwater OK 74078-3035. Tel.: (405) 744-6200, FAX: (405) 744-7799, E-mail: rmatts@biochem.okstate.edu.

[1] Abbreviations: 90 kDa heat shock protein, Hsp90; Cdc37, generically used to refer to the protein product of *CDC37* gene homologues regardless of source of organism; HRI, heme-regulated eIF2α kinase; eIF, eukaryotic initiation factor; eIF2 α, α-subunit of eukaryotic initiation factor 2; EDTA, ethylenediamine tetraacetic acid; IgG, imunoglubulin G; IgM, immunoglobulin M; SDS−PAGE, sodium dodecyl sulfate−polyacrylamide gel electrophoresis; PIPES, piperazine-*N*,*N*′-bis[2-ethanesulfonic acid]; PP5, phosphoprotein phosphatase 5; TPR, tetratricopeptide repeat; FKBP, FK506 binding protein; DMSO; dimethyl sulfoxide; PVDF; poly(vinylidene difluoride); PCR, polymerase chain reaction.

10.1021/bi035001t CCC: $25.00 
Published on Web 10/11/2003

postulated "chaperone" sites (reviewed in refs *1*−*8*). Current models suggest that co-chaperones facilitate the binding of Hsp90 to client targets and confer specificity to this process (*28*, *30*, *31*). One such Hsp90 co-chaperone, namely, Cdc37, interacts with immature forms of Hsp90-dependent kinases, and provides a biochemical activity that is essential for Hsp90-mediated support of kinase function (e.g., refs *20*, *38*−*41*). Although Cdc37 interactions were initially thought to be specific to heterocomplexes formed between Hsp90 and protein kinases, subsequent work has shown that Cdc37 is present in Hsp90 complexes containing the androgen receptor (*42*) and reverse transcriptase (*43*), suggesting a more diverse set of client targets for Cdc37.

In vitro, Cdc37 exhibits chaperone activity similar to Hsp90, preventing the aggregation of denatured protein and maintaining denatured protein in an activation-competent state (*38*). Other Hsp90 co-chaperone partners, such as FKBP52, Cyp40 and p23, similarly exhibit chaperone activity in vitro (*44*, *45*). Like Hsp90, the basis for the recognition of denatured protein by these co-chaperones is unknown.

Hsp90 inhibitors represent powerful tools for dissecting the mechanisms underlying Hsp90 function (*7*, *46*). Hsp90's N-terminal nucleotide binding domain is the site of action for the Hsp90 inhibitor geldanamycin (*47*−*49*). Analyses with this compound, with nucleotides and nucleotide analogues, and with site-direct mutants have revealed that Hsp90 function is regulated via the binding and hydrolysis of ATP (reviewed in refs *2* and *3*), which mediates essential global switching between at least two alternative Hsp90 conformations (reviewed in refs *2* and *3*). In the presence of geldanamycin, Hsp90 binds weakly to client kinases, while Hsp90's "late" co-chaperones, such as Cdc37, immunophilins, and p23, are absent (*13*, *41*). These aberrant Hsp90 heterocomplexes indicate that nucleotide-regulated conformational switching is required to generate high affinity interactions within Hsp90/Cdc37-kinase heterocomplexes (*13*, *41*).

A second ATP binding site has been identified to reside within the middle to C-terminal region of Hsp90 (*50*−*52*). This region of Hsp90 appears to mediate the interaction of Hsp90 with molybdate (*52*, *53*), may contain a site for interaction of Hsp90 with protein clients (*30*), and modulates the ATPase activity of Hsp90's N-terminal nucleotide binding domain (*54*). Like geldanamycin, molybdate inhibits Hsp90. In contrast to geldanamycin, however, this inhibition reflects the "locking" or freezing of Hsp90-kinase complexes, causing the accumulation of Hsp90 complexes containing the Hsp90 co-chaperone p23 and an assortment of other "late" co-chaperones, such as Cdc37 and immunophilins (*13*, *41*, *53*, *55*−*59*). Consistent with this "locking" mechanism for molybdate action, molybdate stabilizes the normally labile interaction of Hsp90 with steroid receptor clients (*13*, *53*). In contrast to receptor clients, however, Hsp90's interactions with kinase clients are stable to high salt concentrations independent of molybdate freezing (*13*, *41*, *53*). Thus, geldanamycin and molybdate have opposing effects on Hsp90-client interactions, demonstrating a link between each compound's effects on Hsp90's nucleotide-mediated conformational switching (*13*, *41*, *53*).

In this report, we dissect the domain structure of two Hsp90 protein kinase clients [the Src-family tyrosine kinase $p56^{lck}$ (Lck) and the heme-regulated eIF2α kinase (HRI)] to identify segments recognized by Hsp90 and Cdc37. The data indicate that Hsp90 and Cdc37 recognize structures or sequences present in the N-terminal lobe of kinase catalytic domains, and that one or more additional motifs present in the C-terminal lobe of the catalytic domain stimulate the nucleotide-dependent conformational switching of Hsp90 that generates molybdate-independent high affinity interactions between Hsp90, Cdc37, and kinase clients.

## EXPERIMENTAL PROCEDURES

*Plasmids.* The coding sequences for protein domains and subdomains were cloned into a modified pSP64T plasmid (*60*) as previously described (*15*, *61*, *62*). N-terminally His-tagged and non-His-tagged versions of each domain were constructed. Sequences represented the Lck catalytic domain (Cat: residues 228−498), the N-terminal lobe of the catalytic domain of Lck (NL: residues 228−323), the C-terminal lobe of the catalytic domain of Lck (CL: residues 317−498), regions of Lck's catalytic domains encompassing conserved kinase motifs I−VIII (NL-APE: residues 228−410), or the regions of Lck's catalytic domain encompassing kinase motifs IV−VIII (*β*4-APE: residues 303−410). These dissections are represented graphically in Figure 1A. Sequences representing the catalytic domain of HRI starting at the third methionine in HRI's coding sequence (Met3; residues 131) or at residue 158 (ΔHBD) of HRI to its C-terminus, the N-terminal heme-binding domain of HRI (HBD: residues 1−158); the N-terminal kinase lobe of HRI (NL: residues158−250); the kinase insertion sequence (KIS: residues 239−387); and the C-terminal lobe the catalytic domain of HRI (CL: residues 387−574) were similarly cloned and are represented graphically in Figure 1B.

*Co-Immunoprecipitations of Chaperones with His-Tagged Kinase Constructs*. Kinase constructs were synthesized and radiolabeled by coupled transcription/translation in nuclease-treated rabbit reticulocyte lysate in the presence of [$^{35}$S]Met at 30 °C for 30 min, followed by a 10-min incubation after the addition of 60 $\mu$M aurintricarboxylic acid to arrest further initiation of protein synthesis (*13*, *41*, *59*, *63*, *64*). His-tagged constructs were adsorbed with anti-His-tag antibody (Qiagen) or a nonspecific control IgG (MOPC21 Sigma) bound to agarose (*65*). Immunoresins were washed 4 times with 10 mM PIPES buffer (pH 7.2) containing 0.5% Tween-20 in the presence or absence of 20 mM molybdate as indicated in the figure legends. Wash regimens were (i) twice with buffer lacking NaCl, once with 50 mM NaCl, and once with buffer lacking NaCl (low stringency wash); (ii) 4 times with buffer containing 150 mM NaCl (medium stringency washes); or (iii) once with buffer containing 50 mM NaCl, twice with buffer containing 500 mM NaCl, and a final wash with buffer containing 50 mM NaCl (high stringency wash). Specific regimens utilized are indicated in the figure legends. Samples were eluted by boiling in SDS sample buffer, separated by SDS−PAGE, and transferred to PVDF membrane for Western blotting and autoradiography. Membranes were stained lightly with Coomassie blue to visualize protein patterns and the molecular weight markers; dried and exposed to film to determine presence and pattern of radioactively labeled protein bands; and then cut according to molecular weight markers for probing with the appropriate anti-chaperone antibodies. Immunoadsorption of each target

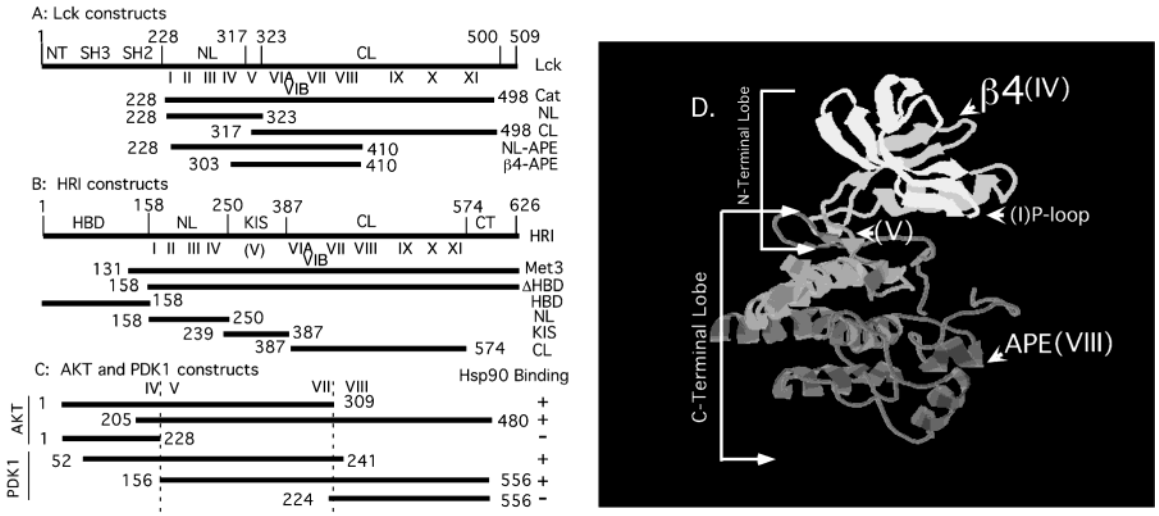


FIGURE 1: Summary of protein kinase constructs used for analysis of Hsp90 and Cdc37 binding. The domain architecture of the Lck (A) and HRI (B) kinases are indicate at the top of their respective sections. The numbers above the lines indicate the amino acids residues that flank: (A) Lck's unique N-terminal domain (NT), SH2 and SH3 domains; Lck's N-terminal (NL) and C-terminal (CL) catalytic lobes, and Lck's C-terminal tail; and (B) HRI's N-terminal heme-binding domain (HBD), HRI's N-terminal (NL) and C-terminal (CL) catalytic lobes; and HRI's kinase insertion sequence (KIS) and C-terminal tail (CT). The Roman numerals below the line indicate the locations of conserved kinase motifs I−XI. In B, (V) indicates that the motif corresponding to the interdomain linker between the catalytic lobes of HRI lies somewhere within the KIS. The lower lines indicate the amino acid residues present in each of the domain and subdomain constructs studied in this report with the abbreviation used to refer to each construct indicated to the right of each line. (C) Lines summarize the amino acid residues present in the constructs of the AKT (*36*) and PDK1 (*35*) kinases that were used to define regions of these kinases that interacted with Hsp90. Hsp90 binding activity (+), or lack thereof (−), of the constructs is indicated at the right of each line. The relative positions of kinase motifs IV, V, VII, and VIII are indicated on the top of the first line. For clarity and to assist in aligning these motifs, the lines are not drawn to exact scale. (D) Ribbon diagram of the crystal structure of the Lck catalytic domain (PDB code 3Lck) created using RasMol2.6. Positions of kinase motifs I, IV, V, and VIII are indicated by the arrows.

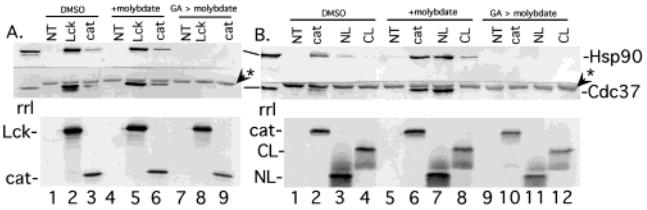


FIGURE 2: Interaction of Hsp90 and Cdc37 with domain and subdomain constructs of Lck. [$^{35}$S]Labeled His-tagged full-length Lck (Lck: A, lanes 2, 5, and 8), Lck catalytic domain (Cat: A, lanes 3, 6, and9; B, lanes 2, 6, and 10), Lck N-terminal kinase lobe (NL: B, lanes 3, 7, and 11), or Lck C-terminal kinase lobe (CL: B, lanes 4, 8, and 12) were synthesized in reticulocyte lysate for 25 min at 30 °C in the presence of DMSO as vehicle control (A: lanes 1−6; B: lanes 1−8) or 10 $\mu$g/mL geldanamycin (GA > molybdate: A, lanes 7−9; B, lanes (10−12). Samples were then supplemented with 20 mM molybdate (+ molybdate or GA > molybdate: A, lanes 4−9; B, lanes 5−12) or buffer (DMSO: A, lanes 1−3; B, lanes 1−4) and adsorbed with anti-His antibodies. Immunoresins were washed at medium stringency with buffer containing 0.05% Tween-20. [$^{35}$S]Labeled Lck constructs and coadsorbing Hsp90 and Cdc37 were detected by autoradiography (lower panels) and Western blotting (upper panels), respectively. A reticulocyte lysate reaction containing no template was assessed as a negative control (NT- A: lanes 1, 4, and 7; B, lanes 1, 5, and 9). rrl: an aliquot of rabbit reticulocyte lysate run as a standard for the detection of Hsp90 and Cdc37. Arrowhead with asterisk points to the immunoreactive heavy chain of the IgG.

kinase construct was confirmed by autoradiography or Western blotting with anti-His antibody, as exemplified in Figure 2.

Radiolabeled PP5 was generated by couple transcription/translation in reticulocyte lysate as previously described and coadsorption of PP5 with kinase constructs was detected by autoradiography (*59*). Hsp90, Cdc37, and Cyclophilin-40 were detected by Western blotting with anti-Hsp90 (*59*), anti-Cdc37 (*13*), or anti-cyclophilin-40 (PA3−003, Affinity BioReagents) polyclonal antiserum. FKBP52 and p23 were immunoadsorbed from reticulocyte lysate with EC1 anti-FKBP52 and JJ3 anti-p23 monoclonal antibodies, respectively, as previously described (*13*, *58*, *65*, *66*).

*Analysis of the Co-Translational Interaction of Hsp90 and Cdc37 with Polyribosomes.* [$^{35}$S]Labeled Firefly luciferase, Lck, and HRI were synthesized by couple transcription/tranlation in nuclease-treated rabbit reticulocyte lysates for 15 min at 30 °C as previously described (*15*, *61*). Protein synthesis reactions were then incubated for an additional 5 min at 30 °C in the presence or absence of 1 mM puromycin. After puromycin treatment, protein synthesis reactions were diluted with 2 volumes of ice-cold buffer containing 20 mM Tris-HCl (pH 7.5), 25 mM KCl, and 2.5 mM magnesium acetate. Samples were layered on top of linear 15−40% sucrose gradients containing 20 mM Tris-HCl (pH 7.5), 25 mM KCl, and 2.5 mM magnesium acetate. Polyribosomes were sedimented by centrifugation for 4.5 h at 150000$g_{av}$ in an AH650 Sorval rotor. The supernatants were removed and ribosomal pellets were dissolved in SDS sample buffer and protein present in the ribosomal pellets were separated by SDS−PAGE, transferred to PVDF membrane, and analyzed by Western blotting as previously described (*41*, *63*).

*Immunoprecipitation of Nascent Lck and HRI Polypeptides.* Protein synthesis reactions that had been treated with 1 mM puromycin, as described above, or treated with 10 mM EDTA were immunoadsorbed with 8D3 anti-Hsp90 monoclonal antibody, OSU anti-Cdc37 polyclonal antibody or nonspecific IgM or IgG antibodies prebound to either goat anti-mouse IgG or goat anti-mouse IgM coupled agarose (*65*). Samples were mixed with the immunoresins for 1 h on ice. Immunoresins were washed at medium stringency.

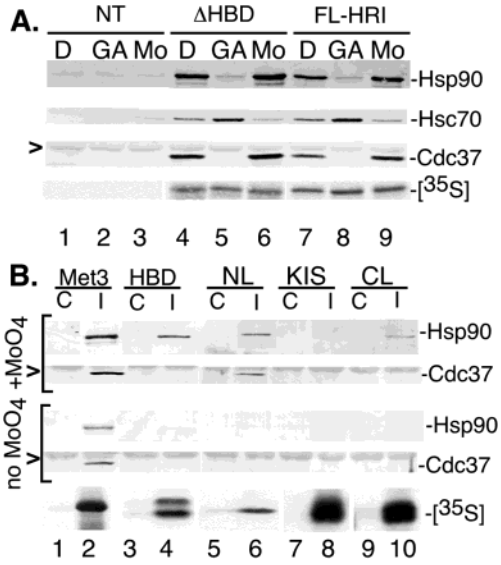


FIGURE 3: Interaction of Hsp90 and Cdc37 with domain and subdomain constructs of HRI. (A) [$^{35}$S]Labeled His-tagged catalytic lobe of HRI (ΔHBD) or full-length HRI (FL-HRI) were synthesized in reticulocyte lysate in the presence of 10 $\mu$g/mL geldanamycin (GA: lanes 2, 5, and 8) or an equal volume of DMSO (D: lanes 1, 4, and 7) for 30 min at 30 °C, followed by immunoadsorption to anti-His-tag antibody resin. Samples containing DMSO were immunoadsorbed in the presence (Mo: lanes 3, 6, and 9) or absence of 20 mM molybdate. Lysate containing no template (NT-control) was immunoadsorbed as a control for nonspecific binding of proteins to the immunoresin. Samples were washed at medium stringency and separated by SDS−PAGE on 8% gels, transferred to PVDF membrane, and Western blotted with anti-Hsp90, anti-Hsc70, or anti-Cdc37 antibodies. [$^{35}$S]: Sections of the autoradiogram of His-tagged [$^{35}$S]labeled HRI products. (B) [$^{35}$S]Labeled His-tagged HRI constructs, HRI/Met3, the N-terminal heme-binding domain (HBD), the N-terminal lobe (NL), the kinase insertion sequence (KIS) and the C-terminal lobe (CL), were synthesized by coupled transcription/translation for 30 min at 30 °C in reticulocyte lysate. The HRI constructs were immunoadsorbed with the anti-His-tag antibody (I: lanes 2, 4, 6, 8, and 10) or nonimune control antibody (C: lanes 1, 3, 5, 7, and 9) in the presence (+$MoO_4$: upper panel) or absence (no $MoO_4$: lower panel) of 20 mM molybdate. Samples were analyzed as described above: Western blot for Hsp90 (−Hsp90) and Cdc37 (−Cdc37). [$^{35}$S]: Sections of the autoradiogram of His-tagged [$^{35}$S]labeled HRI constructs immunoadsorbed from reticlocyte lysate reactions in the absence of molybdate. Similar amounts of HRI constructs were adsorbed in the presence of molybdate (not shown).

Bound proteins were eluted by boiling in SDS sample buffer, separated by SDS−PAGE on 10% polyacrylamide gels, transferred to PVDF membrane, and analyzed by autoradiography.

## RESULTS

*Identification of Conserved Subdomains of Lck and HRI that Interact with Hsp90 and Cdc37.* Hsp90 and Cdc37 primarily recognize and interact with the catalytic domain of protein kinases (*35*, *36*, *40*, *67*−*70*). Therefore, N-terminally His-tagged catalytic domains of Lck (Cat) and HRI (ΔHBD) were cloned and expressed by coupled transcriptional/translation in nuclease-treated reticulocyte lysate. The domains were then immunoadsorbed with anti-His antibodies and analyzed by SDS−PAGE and Western blotting for coadsorbing chaperones. Consistent with previous findings, immunoadsorption of the kinase domains of Lck [Figure 2A (Cat)] and HRI [Figure 3A (ΔHBD)] coadsorbed Hsp90 and Cdc37. The specificity of these coadsorptions was confirmed by the lack of chaperone binding in the absence of kinase gene products, or in the presence of the Hsp90 inhibitor geldanamycin. Notably, the interactions of Hsp90 and Cdc37 with kinase catalytic domains were stable to washing with high ionic strength buffers in the absence of molybdate and were only moderately enhanced by this compound [Lck (Figure 2A), HRI (Figure 3A)].

To further delineate kinase segments that interacted with Hsp90 and Cdc37, we utilized the known crystal structures of protein kinases as a guide to express discrete subdomains of the kinases (Figure 1). The N-terminal heme-binding domain (HBD) of HRI, the N-terminal (NL) and C-terminal catalytic lobes (CL) of HRI and Lck, and the 130-residue kinase insertion sequence separating the N- and C-terminal lobes of HRI (KIS) were expressed in reticulocyte lysate and immunoadsorbed via an N-terminal His-epitope tag. SDS−PAGE and autoradiography confirmed the expression and immunoadsorption of [$^{35}$S]labeled Lck (Figure 2B) and HRI (Figure 3B) gene products. Western blot analysis indicated that in the absence of molybdate, HRI's HBD and KIS (Figure 3B), and the N-terminal and C-terminal catalytic lobes of HRI (Figure 3B) and Lck (Figure 2B) showed little (Lck NL, HBD) or no interaction with either Hsp90 or Cdc37 above that observed for the negative control lanes.

In contrast to interactions observed in the absence of molybdate, Hsp90 and Cdc37 were strongly coadsorbed with the N-terminal catalytic lobes of both HRI and Lck in the presence of molybdate (Figures 2B and 3B). To a lesser extent, molybdate stimulated the recovery of Hsp90 with the kinases' C-terminal lobes, but Cdc37 was nonetheless absent despite the excellent sensitivity of the anti-Cdc37 antibodies employed (Figures 2B and 3B). As controls for specificity of binding, the interaction of Hsp90 and Cdc37 with the N-terminal lobes of the kinases was inhibited by prior treatment of the reticulocyte lysate reactions with geldanamycin (Figures 2A and 4A). Similarly, geldanamycin also inhibited the interaction of Hsp90 with HBD of HRI (Figure 4B). These observations provided strong evidence that the N-terminal catalytic lobe of kinases was the primary target of Cdc37 binding.

The resistance of individual interactions to washing with high ionic strength buffers was noteworthy. In the absence of molybdate, client interactions with Hsp90 and Cdc37 were salt-resistant only for the full-length kinases and their respective catalytic domains (Figures 3 and 4 and refs *13* and *41*). However, deletion of either lobe of the kinase's catalytic domains produced chaperone−client heterocomplexes that were salt-labile and required molybdate for stabilization. Thus, while the N-terminal catalytic lobes of HRI and Lck appear to contain the primary recognition motif for their interaction with Hsp90 and Cdc37, additional sequence in the C-terminal lobes of the catalytic domains were necessary to form the typical salt-resistant chaperone−client heterocomplex.

Hsc70 is required for the assembly of "early" stage complexes between Hsp90 and client proteins (e.g., steroid hormone receptors; *71*−*74*), and is required for the maturation of HRI into an active kinase (*64*, *75*). Geldanamycin causes the accummulation of early stage low affinity Hsp90−client complexes (*13*, *15*, *41*) that are enriched in Hsc70 (*55*, *76*−*80*), as it inhibits the progression of Hsp90 through its

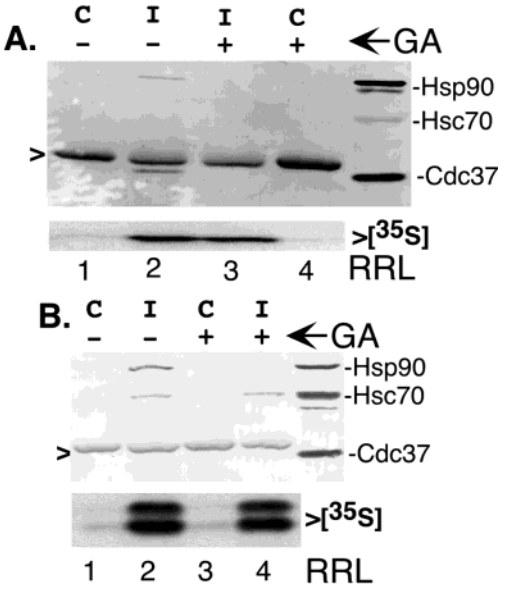


FIGURE 4: Effect of geldanamycin on the interactions of Hsp90 and Cdc37 with the N-terminal catalytic lobe and the heme-binding domain of HRI. [35S]Labeled His-tagged N-terminal lobe of HRI's kinase domain (A) or HRI's N-terminal heme-binding domain (B) were synthesized in reticulocyte lysate in the presence of 10 $\mu$g/mL geldanamycin (+: lanes 3 and 4) or an equal volume of DMSO (−: lanes 1 and 2) for 30 min at 30 °C. Samples were immunoadsorbed with anti-His-tag antibody (I: A, lanes 2 and 3; B, lanes 2 and 4) or an equivalent amount of nonimmune control mouse IgG antibody (C: A, lanes 1 and 4; B, lanes 1 and 3) resin. Samples washed at medium stringency and were analyzed as described above and Western blotted to detect coadsorption of Hsp90, Hsc70, and Cdc37. >: antibody heavy chain. [35S]: Sections from the autoradiogram of immunoadsorbed His-tagged [35S]labeled HRI constructs.

ATP-driven reaction cycle (reviewed in ref *4*). Consistent with the role of Hsc70 in assembly of Hsp90−client complexes and the effect of geldanamycin of Hsp90 function, an increase in the amount of Hsc70 coadsorbing with full-length HRI and its catalytic domain was observed in the presence of geldanmycin (Figure 3A). Similarly, while geldanamycin inhibited the interaction of Hsp90 with the HBD of HRI, it did not inhibit the interaction of Hsc70 with the HBD (Figure 4B). These results are consistent with a role for Hsc70 in the assembly of the Hsp90 chaperone complex with these specific domains, as opposed to Hsc70 simply recognizing the construct as misfolded proteins.

*Identification of Motifs Required for Stable Molybdate-Independent Binding of Hsp90 and Cdc37 to Kinase Catalytic Domains.* To further delineate segments recognized by Hsp90 and Cdc37, two additional Lck deletion mutants were constructed (see Figure 1). Construct "NL-APE" contained the N-terminal Lck kinase lobe plus sequences of the kinase's C-terminal lobe through the APE box (aka motif VIII). Construct "$\beta$4-APE" contained only the $\beta$4-sheet (motif IV) of the N-terminal lobe, the $\beta$5-sheet+interdomain-linker region (motif V) between the two lobes, and segments of the C-terminal kinase lobe through the APE box (motif VIII) (Figure 1A). These constructions were guided by known kinase crystal structures and by previous studies that hypothesized that the region of protein kinases between motifs IV-XIII might be sufficient to specify Hsp90-binding (*35*, *36*). Similar rationally designed constructs cannot be made for HRI, because the KIS is located between the two

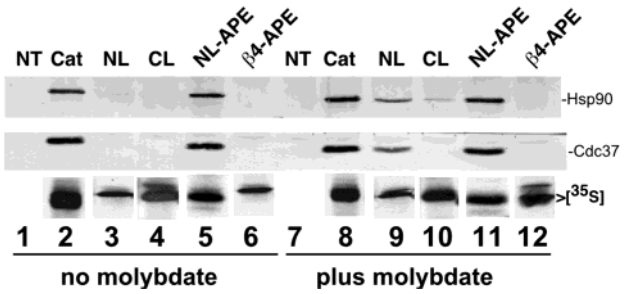


FIGURE 5: Identification of Lck constructs that maintain salt-stabile molybdate-independent binding to Hsp90 and Cdc37. [35S]Labeled His-tagged catalytic domain (Cat: lanes 2 and 8), N-terminal kinase lobe (NL: lanes 3 and 9), C-terminal kinase lobe (lanes 4 and 10), NL-APE Lck construct (lanes 5 and 11) and $\beta$4-APE construct (lanes 6 and 12) were synthesized for 25 min in reticulocyte lysate at 30 °C followed by the addition (plus molybdate, lanes 7−12) or not (no molybdate lanes 1−6) of 20 mM molybdate. The samples were then immunoadsorbed with anti-His-tag antibody. Immunoresins were then washed at high stringency (buffer containing 0.5 M NaCl). Samples were analyzed by Western blotting for coadsorbed Hsp90 (upper panel) and Cdc37 (lower panel). >[35S]: Sections from the autoradiogram of immunoadsorbed His-tagged [35S]labeled HRI constructs. NT: Lysate containing no template as control for nonspecific binding of Hsp90 and Cdc37 to resin in the presence (lanes 7) or absence, (lane 1) of 20 mM molybdate.

subdomains of its kinase catalytic domain, thus hindering definitive structural predictions.

When these Lck dissections were analyzed, both Hsp90 and Cdc37 were found to form salt-stabile complexes with NL-APE. Importantly, molybdate was not necessary for the stabilization of these complexes, and NL-APE chaperone complexes were detected in the absence of molybdate with efficiencies similar to that of the heterocomplexes formed between Hsp90−Cdc37 and the kinase catalytic lobe (Figure 5). Thus, a segment of kinase that was present on NL-APE but absent on NL *triggered* formation of the native salt-stable chaperone−client heterocomplex.

This molybdate-independent binding of Hsp90−Cdc37 to NL-APE (Figure 5) versus their molybdate-dependent binding to NL (Figures 2 and 3), and the molybdate-dependent binding of Hsp90 to the isolated C-terminal kinase domain (Figures 2 and 3), together with hypotheses proposed in previous studies carried out on the AKT and PDK1 kinases (*35*, *36*), predicted that the kinase segments distinguishing NL from NL-APE might bind Hsp90. However, no binding of Hsp90 to the isolated $\beta$4-APE segment was apparent in the absence of molybdate, and the binding observed in the presence of molybdate was less than 3% of that observed with the catalytic domain or the NL-APE construct (Figure 5). Furthermore, no interaction of Cdc37 was observed with the $\beta$4-APE mutant. Thus, while the segment from kinase motifs V to VIII (unique to NL-APE versus NL) contained the *trigger* that caused Hsp90−Cdc37 to assume the molybdate-independent client-binding conformation, the biochemical entities (e.g., the specific component(s) of the Hsp90 chaperone machine) responsible for binding and recognizing this trigger could not be definitively assigned.

*Interaction of Other Hsp90 Co-Chaperones with the Catalytic Domains and Subdomains of Lck and HRI.* The Hsp90 chaperone machine includes various parnter co-chaperones, including, FKBP52, cyclophilin 40 (Cyp40), protein phosphatase 5 (PP5), and p23. Each of these co-chaperones is also present in Hsp90−Cdc37 heterocomplexes

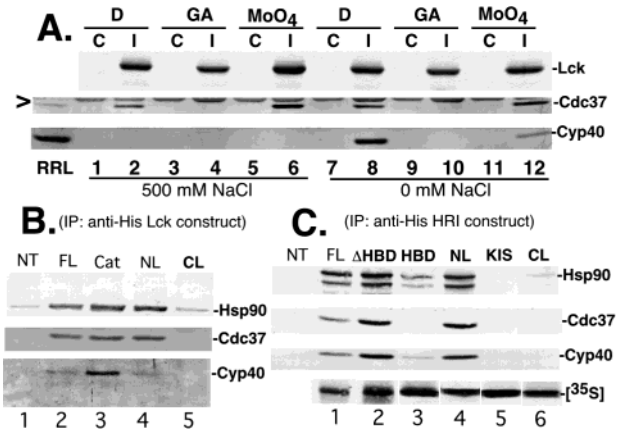


FIGURE 6: Interaction of Cyp40 with domain and subdomain constructs of Lck. (A) [$^{35}$S]Labeled His-tagged Lck was synthesized in reticulocyte lysate in the presence of 10 $\mu$g/mL geldanamycin (GA: lanes 3, 4, 9, and 10) or an equal volume of DMSO (D: lanes 1, 2, 7, and 8) for 20 min at 37 °C. Samples were immunoadsorbed with anti-His-tag antibody (I: lanes 2, 4, 6, 8, 10, and 12) or an equivalent amount of nonimmune control mouse IgG antibody (C: lanes 1, 3, 5, 7, 9, and 11) resin. Samples containing DMSO were immunoadsorbed in the presence ($MoO_4$: lanes 5, 6, 11, and 12) or absence of 20 mM molybdate. Resins were washed at high stringency (500 mM NaCl: lanes 1−6) or low stringency (0 mM NaCl: lanes 7−12). Samples were separated by SDS−PAGE and transferred to PVDF membrane. Adsorbed [$^{35}$S]labeled His-tagged Lck was detected by autoradiography (upper panel) and coadsorbed Cdc37 (middle panel) and Cyp40 (lower panel) were detected by Western blotting. RRL, rabbit reticulocyte lysate, used a standard for protein detection. His-tagged [$^{35}$S]labeled full-length Lck (FL, lane 2), Lck catalytic domain (Cat, lane 3), N-terminal kinase lobe (NL lane 4), or C-terminal kinase lobe (CL lane 5) (B), or full-length HRI (FL, lane 1), HRI catalytic domain (ΔHBD, lane 2), HBD (HBD, lane 3), N-terminal kinase lobe (NL lane 4), kinase insertion sequence (KIS, lane 5), or C-terminal kinase lobe (lane 6) (C) were synthesized in reticulocyte lysate for 20 min at 37 °C. Reactions were supplemented with 20 mM sodium molybdate, clarified and immunoadsorbed with anti-His-tag antibody, and resin washed at low stringency. Samples were analyzed by SDS−PAGE, and Western blotting to detect coadsorbed Hsp90, Cdc37, and Cyp40. Lysate containing no template (NT) was immunoadsorbed as a control for nonspecific binding of proteins to the immunoresin. [$^{35}$S]: autoradiogram of [$^{35}$S]labeled His-tagged HRI translation products. Lck translations were quantified by measuring the amount of [$^{35}$S] incorporated into acid precipitable translation products, and equivalent molar amounts of translation products were loaded in each lane.

containing client kinases HRI and Lck (Figures 6−8 and refs *13*, *59*, and *65*).

To determine the kinase segments that might mediate the recruitment of these co-chaperones to the kinase−Hsp90−Cdc37 complex, the various Lck and HRI constructs described above (see Figure 1) were assayed for concomitant binding of co-chaperones. As previously described, Cyp 40 was associated with full-length Lck (Figure 6A) and HRI (Figure 6C). Like the binding observed for Hsp90 and Cdc37, the binding of Cyp40 to Lck was sensitive to treatment with geldanamycin (Figure 6A). In contrast to Hsp90 and Cdc37, however, Cyp40 binding to Lck and to full-length HRI (not shown) was salt-labile even in the presence of molybdate. Indeed, the higher ionic strength represented by the addition of 20 mM molybdate to the wash buffer was sufficient to dissociate a significant amount of Cyp40 from complexes formed between Hsp90, Cdc37, and Lck. Thus, the interaction of the Cyp40 immunophilin with Hsp90−client complexes differs from that of Cdc37: Cyp40 is an inherently

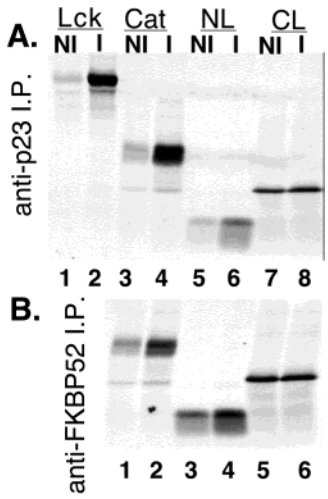


FIGURE 7: Interaction of p23 (A) and FKBP52 (B) with domain and subdomain constructs of Lck. [$^{35}$S]Labeled His-tagged full-length Lck (A: FL, lanes 1 and 2), Lck catalytic domain (Cat: A, Cat lanes 3 and 4: B, lanes 1 and 2), Lck N-terminal kinase lobe (NL: A, lanes 5 and 6; B: lanes 3 and 4), and Lck C-terminal kinase lobe (CL: A, lanes 7 and 8; B, lanes 5 and 6) were synthesized in reticulocyte lysate cDNAs for 20 min at 37 °C reactions. Samples were supplemented with 20 mM $Na_2MoO_4$, clarified by centrifugation, and mixed with immunoresins preabsorbed with JJ3 anti-p23 monoclonal antibody (I: A, lanes 2, 4, 6, and 8), EC1 anti-FKBP52 monoclonal antibody (I: B, lanes 2, 4, and 6), or the nonimmune IgG antibody (NI: A and B odd-numbered lanes). Immunoresins were washed at low stringency and were analyzed by SDS−PAGE and autoradiography for coadsorption with p23 (A) and FKBP52 (B).

labile component of these complexes whose binding did not appear to be stabilized by molybdate.

Immunoadsorption of truncated Lck gene products demonstrated that the association of Cyp40 with Lck was governed by the Lck catalytic domain, and did not require the kinase's regulatory SH2 or SH3 domains (Figure 6B). Further dissection of Lck revealed that Cyp40 interacted with the N-terminal but not the C-terminal lobe of the catalytic domain. Additionally, Cyp40 was observed to coadsorb with the catalytic domain, the HBD, and the N-terminal catalytic lobe of HRI, but not the C-terminal catalytic lobe or HRI's KIS subdomain of HRI (Figure 6C). While the interaction of Cyp40 with the full-length constructs and catalytic domains of HRI and Lck, and the HBD of HRI was detected using low stringency washes in the absence of molybdate, addition of molybdate was required to detect the interaction of Cyp40 with the N-terminal catalytic lobes of the kinases (not shown).

To investigate the interaction of FKBP52 and p23 with Lck constructs, FKBP52 or p23 were immunoadsorbed from reticulocyte lysate using EC1 anti-FKBP52 or JJ3 anti-p23 monoclonal antibodies, and the presence of coadsorbing [$^{35}$S]-Lck kinase constructs was analyzed by SDS−PAGE and autoradiography. This approach was utilized because the EC1 and JJ3 antibodies used in this study lacked the sensitivities to efficiently detect levels of their respective co-chaperone antigens present in Lck heterocomplexes. EC1 anti-FKBP52 antibodies (Figure 7B) and JJ3 anti p23 antibodies (Figure 7A) coadsorbed the full-length, catalytic domain, and N-terminal kinase lobe constructs of Lck in an immune specific fashion. The experiment with C-terminal kinase lobe was compromised, however, by high levels of nonspecific bind-

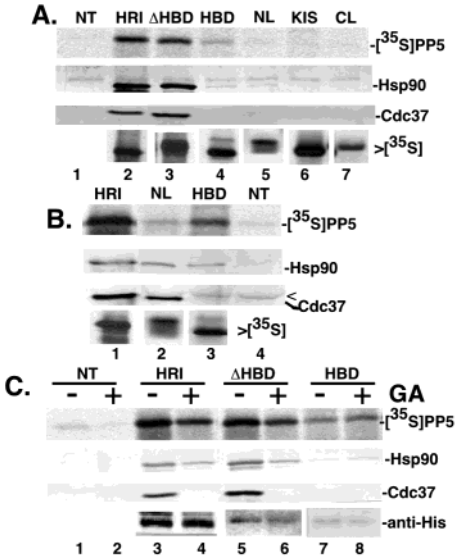


FIGURE 8: Interaction of PP5 with domain and subdomain constructs of HRI. [35S]Labeled His-tagged full-length HRI (HRI: A, lane 2; B, lane 1), catalytic domain (ΔHBD: A, lane 3), N-terminal heme-binding domain (HBD: A, lane 4; B, lane 3), N-terminal kinase lobe (NL: A, lane 5; B, lane 2), kinase insertion sequence (KIS: A, lane 6), and C-terminal kinase lobe (CL: A, lane 7) were synthesized in reticulocyte lysate for 30 min at 30 °C as described under Experimental Procedures. The reactions were then mixed at a 1:1 ratio with reticulocyte lysate containing newly synthesized FLAG-[35S]PP5 and incubated for 20 min. Reticulocyte lysate reaction containing no template plasmid was mixed with an equal volume of FLAG-[35S]PP5-containing lysate to assess the nonspecific binding of proteins (NT: A, lane 1; B, lane 4). Resulting lysate mixtures were subsequently immunoadsorbed to anti-His-tag antibody resin in the presence (B) or absence (A) of 20 mM molybdate. Samples were separated by SDS−PAGE, and transferred to PVDF membrane. Coadsorbed [35S]labeled FLAG-PP5, and Hsp90 and Cdc37 were visualized by autoradiography and Western blotting, respectively. >[35S]: Sections from the autoradiogram of immunoadsorbed His-tagged [35S]labeled HRI constructs. (C) [35S]Labeled His-tagged full-length HRI (HRI), HRI's catalytic domain (ΔHBD), and HRI's N-terminal heme-binding domain (HBD) were synthesized in reticulocyte lysate in the presence (lanes 2, 4, 6, and 8) or absence (lanes 1, 3, 5, and 7) of 10 $\mu$g/mL geldanamycin for 30 min. Reactions without cDNA template (NT) were similarly incubated in the presence (+: lane 2) or absence (−: lane 1) of geldanamycin. Samples were then mixed in a 1:1 ratio with reticulocyte lysate containing synthesized FLAG-[35S]-PP5 and incubated for 20 min with geldanamycin maintained at a concentration of 10 $\mu$g/mL (even-numbered lanes). Samples werre immunoadsorbed to anti-His-tag antibody resin and analyzed as described above. Coadsorption of FLAG-[35S]PP5 (upper panel), and Hsp90 (middle panel), and Cdc37 (lower panel) were analyzed by autoradiography and Western blotting, respectively. His-tagged HRI constructs were detected by Western blotting with anti-His antibody (-anti-His). All immunoresins were washed at high stringency.

ing, and no conclusion could be drawn about the potential interaction of these Hsp90 co-chaperones with the C-terminal kinase lobe of Lck. High levels of nonspecific binding also compromised similar experiments carried out with the individual domains of HRI. Nonetheless, the data allowed us to conclude that p23 and FKBP52, like Cdc37, were present in chaperone hetercomplexes recognizing Lck's N-terminal kinase lobe. Similar to the interaction of Cyp40 with Lck, FKBP52 binding to Lck products was salt-labile and could not be stabilized by addition of molybdate (not shown).

Recently, we have demonstrated that the Hsp90 TPR partner, protein phosphatase 5 (PP5), interacts with HRI and regulates its maturation (*59*). To ascertain which domains of HRI mediate recruitment of PP5 to the HRI−chaperone heterocomplex, [35S]PP5 was synthesized in reticulocyte lysate and mixed with reticulocyte lysates containing epitope-tagged HRI gene products: the radioisotopic labeling strategy was utilized to enhance the sensitivity of the assay (*59*).

[35S]PP5 was specifically coadsorbed with full-length HRI, confirming previously documented interactions between these proteins (Figure 8). This interaction was mediated by the kinase's catalytic domain, as PP5 was coadsorbed by the HRI construct HRI/ΔHBD. Surprising, however, PP5 also bound to the regulatory heme-binding domain of HRI (Figure 8). Little, if any, PP5 was specifically coadsorbed with the N-terminal lobe, KIS, or C-terminal lobe constructs of HRI. Consistent with our previously reported observations with full-length HRI, geldanamycin only partially compromised the interaction of PP5 with the HBD and HRI/ΔHBD constructs. Thus, PP5 recognized the Hsp90-dependent HRI kinase via a complex mechanism that did not entirely correlate to that utilized by Hsp90 and its other cohorts. Although PP5 is also present in chaperone heterocomplexes containing Lck, we have not observed any functional consequences for this interaction (B. Scroggins and R. Matts, unpublished observations), and thus these interactions were not characterized further.

*Interaction of Hsp90 and Cdc37 with Nascent Protein Kinase Polypeptides.* Previously, we have demonstrated that both Hsp90 and Cdc37 interact with nascent HRI co-translationally (*15*, *41*). The ribosome has been estimated to mask as little as 23 and up to as many as 80 amino acids in the pore between its peptidyl-transferase center and the surface of the ribosome (*81*−*83*). Since the NL-APE segments of Lck are approximately 100 amino acids from Lck's C-terminus, the known structure of the ribosomal machinery in conjunction with the observed effect of deleting Lck's C-terminal sequences predicted that Hsp90 and Cdc37 should bind to Lck polyribosomes, unless Lck's Hsp90/Cdc37 interacting motifs were masked through interactions with other lysate components, or are unable to undergo folding events on the ribosomal surface required for Hsp90/Cdc37 binding. Therefore, we compared the ability of Hsp90 and Cdc37 to associate with HRI and Lck co-translationally. Additionally, lysate programmed to synthesize firefly luciferase, which folds independent of Hsp90 (*84*), was used as a negative control.

Consistent with our previous results (*15*, *41*), Hsp90 and Cdc37 were associated with the polyribosomal pellet prepared from lysate programmed to synthesize HRI (Figure 9). The association of Hsp90 and Cdc37 with nascent HRI polypeptide chains was specific, as these proteins were absent from polyribosomal pellets prepared after treatment of reticulocyte lysate with puromycin to release nascent chains from the ribosomes. In dramatic contrast, however, Hsp90 and Cdc37 were not detected in polyribosomal pellets prepared from lysate programmed to synthesize Lck. This result implied that Lck segments recognized by Hsp90−Cdc37 were not available for binding during the actual synthesis of Lck.

To further investigate the capacity of nascent chains of Lck to interact with Hsp90 and Cdc37, we examined the

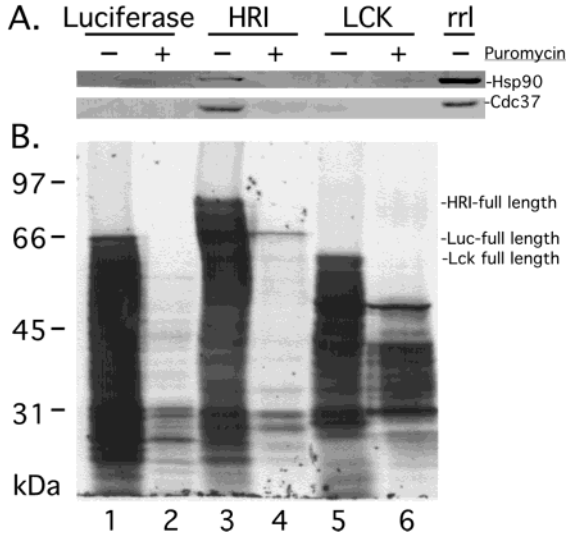


FIGURE 9: Chaperone associations with translating ribosomes. Nuclease treated reiculocyte lysate was programmed with plasmids coding for the synthesis of firefly luciferase (lanes 1 and 2), HRI (lanes 3 and 4), or Lck (lanes 5 and 6). Protein was synthesized for 15 minutes at 30 °C in the presence of [$^{35}$S]methionine. Protein synthesis reactions were then either treated (lanes 2, 4, and 6) or not treated (lanes 1, 3, and 5) with 1 mM puromycin for 5 min to release nascent polypeptides from the translating ribosomes. Polyribosomes were isolated by centrifugation through a 15 to 40% sucrose gradient as described in Experimental Procedures. Components of the polyribosome complex were separated by SDS−PAGE in a 10% gel and blotted to a PVDF membrane. The membrane was analyzed by (A) Western blotting with antibodies against Hsp90, or Cdc37 and (B) by exposure to film for detection of [$^{35}$S]labeled nascent polypeptide. A total of 2 $\mu$L of RRL (lane 7) was used as a standard for immunodetection.

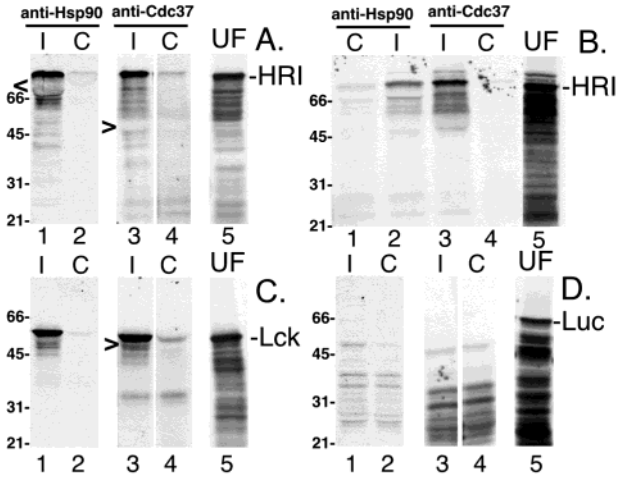


FIGURE 10: Co-immunoprecipitation of nascent polypeptides with anti-Hsp90 and anti-Cdc37 antibodies. Nuclease-treated reticulocyte lysate was programmed with plasmids coding for the synthesis of HRI (A, B), Lck (C), or firefly luciferase (D). Polypeptides were synthesized for 15 min at 30 °C in the presence of [$^{35}$S]methionine. Protein synthesis reactions were then treated with 1 mM puromycin (A, C, and D) or 5 mM EDTA (B) for 5 min at 30 °C to release nascent polypeptides from the translating ribosomes. Equal aliquots of the protein synthesis reactions were immunoadsorbed as described in Experimental Procedures with either anti-Hsp90 monoclonal IgM antibody (I: lane 1 A, C, and D; or lane 2 B) or a nonimmune IgM (C: lane 2 A, C, and D; or lane 1 B) as a control, or anti-Cdc37 antibody (I: lane 3 A, B, C, and D, or nonimmune IgG (C: lane 4 A, B, C, and D) as a control. Two microliters of each of the protein synthesis reactions was loaded (UF) to show the population of polypeptides present in each immunoprecipitation.

ability of anti-Hsp90 and anti-Cdc37 antibodies to coadsorb nascent chains of Lck, HRI, or luciferase that had been released from ribosomes by treatment of reticulocyte lysate with puromycin or EDTA (Figure 10). The molecular dissections of Lck structure and the binding of Hsp90−Cdc37 thereto predicted that only those puromycyl-polypeptides of HRI or Lck containing sequences flanking motifs VII or VIII (HRI products with $M_r$ > 51 kDa) and Lck products with $M_r$ > 43 kDa) would form stable complexes with Hsp90 and Cdc37 independent of the presence of molybdate. Furthermore, since both Cdc37 and nucleotide-modulated conformational switching of Hsp90 are required for the formation of Hsp90/Cdc37 complexes with kinase constructs that are stable in the absence of molybdate, the pattern of [$^{35}$S]puromycyl-polypeptides that are coadsorbed by anti-Hsp90 and anti-Cdc37 would be predicted to be very similar.

As predicted, the distribution of the [$^{35}$S]polypeptides of HRI and Lck that were coadsorbed by the Hsp90 and Cdc37 antibodies were very similar, taking into consideration the distortion of the electrophoretic mobility of bands that comigrated with the heavy chain of the anti-Hsp90 IgM and anti-Cdc37 IgG antibodies. Two higher molecular weight luciferase polypeptides (one just barely visible at 65 kDa) appeared to coadsorb specifically with Hsp90 (Figure 10C). However, consistent with Cdc37's binding specificity for sequences or structures present in protein kinases, no luciferase polypeptides specifically coadsorbed with anti-Cdc37 antibodies. The apparent specific interaction of luciferase puromycyl-polypeptides with Hsp90 is likely due to its previously characterized binding to thermally denatured luciferase molecules (*58*, *85*, *86*). While newly synthesized luciferase has been demonstrated to fold independent of Hsp90 (*84*), luciferase is unstable above 28 °C and luciferase molecules containing C-terminal deletions are even more thermally unstable (*87*).

Compared to the total distribution of [$^{35}$S]labeled polypeptides released from ribosomes, only those nascent polypeptides chains of HRI (Figure 10A,B) and Lck (Figure 10C) with estimated molecular weights sufficient to account for completion of the synthesis of kinase molecules that included motif VIA were coadsorbed with Hsp90 or Cdc37 antibodies. Some HRI puromycyl-peptides with $M_r$ of less than 51 kDa coadsorbed with Hsp90 and Cdc37 (Figure 10A). However, coadsorption of these lower molecular weight peptides was not observed when [$^{35}$S]HRI peptides were released from the ribosome with EDTA (Figure 10B). This result suggests that motifs V−VIII may not represent the "minimal" segment within the C-terminal kinase lobe that is required to trigger Hsp90 conformational switching.

## DISCUSSION

Data presented here indicate that the Hsp90−Cdc37 heterocomplex binds to kinase molecules primarily via the specific recognition of kinase sequence or structure present in the N-terminal lobe of the kinase catalytic domain of Lck and HRI kinases (Figures 2 and 3). This conclusion is supported by three observations: (i) Hsp90−Cdc37 binding to the N-terminal lobe of the catalytic domain is retained upon deletion of the accompanying C-terminal lobe; (ii) Cdc37 binding to the catalytic domain of Lck and HRI is lost when the N-terminal lobe of this domain is deleted; and (iii) puromycyl-peptides of Lck and HRI with molecular

weights sufficient to account for the synthesis of segments that include the majority of the kinase domain of each kinase were the major polypeptides coadsorbed by anti-Hsp90 and anti-Cdc37 antibodies.

This conclusion is consistent with previous conclusions reached regarding binding of Hsp90 to kinase catalytic domains (e.g., *68*). Our biochemical analyses are also consistent with the interaction of Cdc37's C-terminal domain with the N-terminal lobe of the Cdc28 kinase in yeast 2-hybrid systems (*88*). However, we and others have previously shown that Cdc37's kinase-binding activity resides in the N-terminal domain of Cdc37 (*40*, *41*), suggesting subtle contradictions between yeast genetic data and biochemical binding assays. It is notable that while the first 30 or so amino acids of Cdc37's N-terminal kinase binding domain exhibit 50% sequence identity and 70% sequence conservation between the yeast and human proteins, only 19% sequence identity is observed overall between these proteins sequences. Furthermore, there is some conflict in the literature on whether yeast Cdc37 directly binds to Hsp90 to form a stable complex (*38*, *42*, *89*−*91*). Thus, caution should be exercised when comparing the properties of the fungal and animal proteins, as these Cdc37s may not interact with the Hsp90 chaperone machine in the same manner. Nonetheless, the biochemical assays presented here argue strongly that the N-terminal lobes of kinases contain the primary binding sites recognized by the Hsp90−Cdc37 partnership.

Our data and the conclusions they support differ subtly from previous studies concluding that Hsp90 recognizes kinases primarily via the region represented between kinase motifs IV to VIII (*35*, *36*). These previous studies utilized deletion mutagenesis and loss of binding as diagnostic criteria to define the putative borders of "the Hsp90-binding motif." We similarly observe that in the absence of molybdate, Hsp90 does not bind tightly to Lck or HRI gene products lacking this region. However, a stable, specific interaction of Hsp90 with abbreviated Lck and HRI constructs lacking kinase motifs VIA through VIII (Figure 1) is observed in the presence of molybdate. Thus, our detailed dissections, in conjunction with the use of the Hsp90 antagonist and stabilizing agent molybdate, suggest that a complex and subtle mechanism underlies binding of Hsp90 chaperone machinery to client kinases. While our data support the notion drawn from these previous studies that Hsp90 machinery recognizes features of kinases lying within the region flanked by motifs IV−VIII, our findings elaborate on this observation by demonstrating that this region is not sufficient alone to specify Hsp90 binding (Figure 5, lanes 6 and 12). Instead, the N-terminal lobe of these kinases is the primary region recognized by Hsp90 and its partner co-chaperone Cdc37.

This localization to the N-terminal kinase lobe is noteworthy. This region of kinases is a well-documented target for stabilization of cyclin-dependent kinases by their partner cyclins (*92*), and for destabilization of kinases by the p27/p21 kinase inhibitors (*93*, *94*). Additional dissections of sequences within the C-terminal kinase lobe that will more finely resolve interactions required to stimulate Hsp90's conformational switching are currently being studied.

In addition to the specific recognition of the N-terminal kinase lobe by Hsp90−Cdc37, Hsp90 also shows versatile binding to other kinase segments. Thus, Hsp90 appears to recognize both lobes of the kinase catalytic domain, as well as other areas within the HRI kinase. These observations suggest that Hsp90 may recognize a broad range of protein motifs, consistent with the broad range of Hsp90 clients observed in vivo. Similarly, the differing specificities of Cdc37−Hsp90 versus Hsp90 lacking this co-chaperone suggest that Hsp90 co-chaperones may be the primary mechanism by which Hsp90 chaperone machinery recognizes sequences or structures specific to individual families of clients. This theme reiterates concepts developed by previous observations regarding Cdc37's apparent client specificity (*2*−*4*).

Previous work has demonstrated that PP5 can coexist with Cdc37 in Hsp90−HRI complexes, and that Cdc37 and PP5 have opposing effects on the maturation of HRI's kinase activity (*41*, *59*). In contrast to Cdc37, PP5 appears to have a bipartite interaction with HRI, recognizing segments in both the N-terminal HBD and the catalytic domain of the kinase. Similar to its interaction with full-length HRI, PP5's interaction with HRI's catalytic and N-terminal HBD domain constructs was stable to washing with high salt, even in the absence of molybdate, and its binding to the domains was only partially sensitive to inhibition by geldanamycin (*41*, *59*). The stability of the interaction of PP5 with HRI supports the notion that PP5 interacts directly with HRI and is not present in Hsp90/kinase heterocomplexes simply due to its interaction with Hsp90. The contrast in the sensitivities of complexes of HRI with PP5 and Cdc37 to geldanamycin-induced disruption or molybdate-induced stabilization (*41*, *59*) suggests that these co-chaperones may interact with protein kinase motifs at different stages in Hsp90's ATP-driven chaperone cycle. It is also noteworthy that PP5 interacted very weakly, if at all with the N-terminal and C-terminal catalytic lobe constructs of HRI. Thus, PP5 may recognize features present in the folded catalytic domain, a notion consistent with our previous findings that pharmacological inhibition of PP5 function during HRI's Hsp90-dependent maturation and activation ("transformation"), leads to HRI's hyperphosphorylation and hyperactivation of HRI's eIF2α kinase activity (*59*). Since hyperphosphorylated HRI is refractory to inhibition by heme (*95*, *96*), PP5 may function under normal physiological conditions to ensure that "transformed" HRI is released from Hsp90 heterocomplexes in a stable and active, yet heme-regulatable conformation.

Cyp40 interacted with both the catalytic domains of Lck and HRI, and the N-terminal catalytic lobes of these kinases. Similar to PP5, Cyp40 was also coadsorbed with the HBD and catalytic domains of HRI. However, in contrast to PP5, the interaction of Cyp40 with both the full-length kinases, and their subdomains was salt-labile, and the interaction between Cyp40 and the N-terminal catalytic lobes of these kinases could not be detected unless molybdate was added to stabilize the interaction of Hsp90 and Cdc37 with these constructs. Thus, the question of whether these kinases contain recognition motifs with which Cyp40 specifically interacts is uncertain, particularly for the interaction observed between Cyp40 and the N-terminal lobes, as the presence of Cyp40 in these complexes may be simply mediated through its interaction with Hsp90.

It is important to note that binding of Cdc37 and Hsp90 to the isolated N-terminal lobe of the kinase catalytic domain

has an absolute requirement for molybdate stabilization, as complexes formed in the absence of this agent are salt-labile. This effect of molybdate is consistent with its previous use as a stabilizer of Hsp90 binding to steroid receptors (*6*). This requirement for molybdate differs notably, however, from the molybdate-independent binding of Hsp90 and Cdc37 to full-length kinases and to their isolated catalytic domains: these larger kinase gene products form molybdate-independent, salt-resistant heterocomplexes with Hsp90-Cdc37 (*13*, *53*). This difference suggests that one or more segments outside the N-terminal lobe of the kinase catalytic domain are required to establish the salt-resistant chaperone complex that results from of nucleotide-modulated conformation switching of Hsp90 (*13*, *41*).

Consistent with this observation, restoration of Lck residues 323−420 to the kinase N-terminal lobe generates a kinase gene product that forms molybdate-independent salt-stable heterocomplexes with Hsp90−Cdc37 (Figure 5). This kinase segment contains motifs V−VIII, including the APE box. Thus, we now identify this region of the kinase client as containing a bona fide "trigger" that the Hsp90 chaperone machine recognizes as a cue to regulate its nucleotide-mediated conformational switching.

The localization of this switching motif/conformational trigger is also noteworthy. This segment of the catalytic domain contains all the residues essential to the binding of ATP and the catalysis of the phosphotransferase reaction. Additionally, superimposing kinase structures in active and inactive conformations indicates that the αC-helix-$\beta$4 loop and the peptide strand connecting the N-terminal and C-terminal catalytic lobes act as a key region for global changes in kinase conformation, with the αC-helix being rather randomly disposed, but with structural elements meeting at a single point, i.e., a "hinge" (*97*). Twisting motions about the hinge affect the relative position of the N-terminal kinase lobe and the αC-helix, and thus the position of the conserve catalytic Lys and Glu residues relative to the catalytic residues present in the C-terminal lobe (*97*). Small perturbations of these structural elements have significant effects on kinase conformation, and allow for variation in mechanisms that regulate kinase activity (*97*). Thus, Hsp90 chaperone machinery appears to recognize and interact with important structural elements that govern kinase functionality. Finally, the APE box is of further speculatory interest, as it contains a universally conserved proline residue. Prolines have been implicated in immunophilin recognition and function, and Hsp90−Cdc37−immunophilin components bind simultaneously to the same regions of immature kinase clients (Figures 6 and 7).

What mechanisms govern Hsp90's switching from low-affinity to high-affinity binding? While our data suggest that the Hsp90 machine is a versatile chaperone that can recognize multiple kinase segments, this broad specificity is refined by Cdc37's highly specific recognition of the N-terminal kinase lobe. However, the Hsp90 chaperone machine also recognizes other discrete kinase segments with distinct biochemical consequences, namely, the "trigger" for high-affinity binding that is encoded by kinase segments lying in the region from motif VIA to VIII. Although the exact mechanism for this recognition has yet to be characterized, it likely occurs via the concurrent or sequential recognition of these multiple individual client segments. Furthermore, this recognition must be *communicated* or coordinated within the Hsp90 chaperone machine. Consistent with this view, previous studies show correlations between discrete nucleotide-mediated changes in Hsp90's conformation and alterations in the mode by which it binds clients (*13*, *53*). Such communication can reasonably be postulated to occur via stimulation or retardation of Hsp90's nucleotide-mediated conformational switching (*41*). This communication may be orchestrated by interactions among Hsp90's individual co-chaperones, a postulation consistent with the impact of co-chaperones on Hsp90's binding and hydrolysis of ATP (*13*, *52*, *54*, *57*, *73*, *74*, *98*−*111*). Alternatively, our data also support models proposing that Hsp90 itself has two chaperone sites (*28*, *30*). While the precise mechanisms remain to be determined, data presented here demonstrate that the Hsp90 chaperone machine recognizes multiple discrete segments of its client kinases, and that this concomitant recognition and the communication thereof drives Hsp90's nucleotide regulated conformational switching (*28*, *30*).

## ACKNOWLEDGMENT

The authors would like to thank Dr. Douglas Melton (Harvard University) for generously providing the Sp64T plasmid DNA, and Dr. Michael Chinkers (U. So. Alabama Col. Med.) for providing the plasmid encoding FLAG-tagged PP5. Geldanamycin was provided by the Drug Synthesis and Chemistry Branch, Developmental Therapeutics Program, Division of Cancer Treatment, National Cancer Institute, NIH. We would like to thank the Sarkey's Biotechnology Research Laboratory (OSU) for oligonucleotide synthesis and DNA sequencing. Polyclonal mouse ascites antibodies against Hsp90 was prepared by the Oklahoma State University Hybridoma Center for the Agricultural and Biological Sciences, and anti-p23 monoclonal antibody was kindly provided by Dr. David Toft (Mayo Medical School, Rochester, MN).

## REFERENCES

1. Pearl, L. H., and Prodromou, C. (2000) *Curr. Opin. Struct. Biol. 10*, 46−51.
2. Pearl, L. H., and Prodromou, C. (2002) *Adv. Protein Chem. 59*, 157−185.
3. Picard, D. (2002) *Cell Mol. Life Sci. 59*, 1640−8.
4. Richter, K., and Buchner, J. (2001) *J. Cell Physiol. 188*, 281−90.
5. Toft, D. O. (1998) *Trends Endocr. Metab. 9*, 238−243.
6. Pratt, W. B., and Toft, D. O. (1997) *Endocr. Rev. 18*, 306−360.
7. Neckers, L. (2002) *Trends Mol. Med. 8*, S55−61.
8. Csermely, P., Schnaider, T., Soti, C., Prohaszka, Z., and Nardai, G. (1998) *Pharmacol. Ther. 79*, 129−168.
9. Bohen, S. P., Kralli, A., and Yamamoto, K. R. (1995) *Science 268*, 1303−1304.
10. Rutherford, S. L., and Zuker, C. S. (1994) *Cell 79*, 1129−1132.
11. Young, J. C., Moarefi, I., and Hartl, F. U. (2001) *J. Cell Biol. 154*, 267−73.
12. Hartson, S. D., Ottinger, E. A., Huang, W., Barany, G., Burn, P., and Matts, R. L. (1998) *J. Biol. Chem. 273*, 8475−8482.
13. Hartson, S. D., Irwin, A. D., Shao, J., Scroggins, B. T., Volk, L., Huang, W., and Matts, R. L. (2000) *Biochemistry 39*, 7631−7644.
14. Hartson, S. D., Barrett, D. J., Burn, P., and Matts, R. L. (1996) *Biochemistry 35*, 13451−13459.
15. Uma, S., Hartson, S. D., Chen, J.-J., and Matts, R. L. (1997) *J. Biol. Chem. 272*, 11648−11656.
16. Scholz, G. M., Hartson, S. D., Cartledge, K., Volk, L., Matts, R. L., and Dunn, A. R. (2001) *Cell Growth Differ. 12*, 409−417.
17. Queitsch, C., Sangster, T. A., and Lindquist, S. (2002) *Nature 417*, 618−24.
18. Rutherford, S. L., and Lindquist, S. (1998) *Nature 639*, 336−342.

19. Bijlmakers, M. J., and Marsh, M. (2000) *Mol. Biol. Cell 11*, 1585−95.
20. Scholz, G., Hartson, S. D., Cartedge, K., Hall, N., Shao, J., Dunn, A. R., and Matts, R. L. (2000) *Mol. Cell. Biol. 20*, 6984−6995.
21. Yorgin, P. D., Hartson, S. D., Fellah, A. M., Scroggins, B. T., Matts, R. M., and Whitesell, L. (2000) *J. Immunol. 164*, 2915−2923.
22. Schnaider, T., Somogyi, J., Csermely, P., and Szamel, M. (1998) *Life Sci. 63*, 949−54.
23. Nieland, T. J., Tan, M. C., Monne-van Muijen, M., Koning, F., Kruisbeek, A. M., and van Bleek, G. M. (1996) *Proc. Natl. Acad. Sci. U.S.A. 93*, 6135−9.
24. Wearsch, P. A., and Nicchitta, C. V. (1997) *J. Biol. Chem. 272*, 5152−6.
25. Vogen, S., Gidalevitz, T., Biswas, C., Simen, B. B., Stein, E., Gulmen, F., and Argon, Y. (2002) *J. Biol. Chem. 277*, 40742−50.
26. Linderoth, N. A., Popowicz, A., and Sastry, S. (2000) *J. Biol. Chem. 275*, 5472−5477.
27. Argon, Y., and Simen, B. B. (1999) *Semin. Cell Dev. Biol. 10*, 495−505.
28. Dalman, F. C., Scherrer, L. C., Taylor, L. P., Akil, H., and Pratt, W. B. (1991) *J. Biol. Chem. 266*, 3482−90.
29. Bodine, P. V., Alnemri, E. S., and Litwack, G. (1995) *Receptor 5*, 117−22.
30. Scheibel, T., Weikl, T., and Buchner, J. (1998) *Proc. Natl. Acad. Sci. U.S.A. 95*, 1495−9.
31. Caamano, C. A., Morano, M. I., Dalman, F. C., Pratt, W. B., and Akil, H. (1998) *J. Biol. Chem. 273*, 20473−80.
32. Giannoukos, G., Silverstein, A. M., Pratt, W. B., and Simons, S. S., Jr. (1999) *J. Biol. Chem. 274*, 36527−36.
33. Kaul, S., Murphy, P. J., Chen, J., Brown, L., Pratt, W. B., and Simons, S. S., Jr. (2002) *J. Biol. Chem. 277*, 36223−32.
34. Xu, M., Dittmar, K. D., Giannoukos, G., B., P. W., and Simons, S. S., Jr. (1998) *J. Biol. Chem. 273*, 13918−13924.
35. Fujita, N., Sato, S., Ishida, A., and Tsuruo, T. (2002) *J. Biol. Chem. 277*, 10346−53.
36. Sato, S., Fujita, N., and Tsuruo, T. (2000) *Proc. Natl. Acad. Sci. U.S.A. 97*, 10832−7.
37. Couette, B., Jalaguier, S., Hellal-Levy, C., Lupo, B., Fagart, J., Auzou, G., and Rafestin-Oblin, M. E. (1998) *Mol. Endocrinol 12*, 855−63.
38. Kimura, Y., Rutherford, S. L., Miyata, Y., Yahara, I., Freeman, B. C., Yue, L., Morimoto, R. L., and Lindquist, S. (1997) *Genes Dev. 11*, 1775−1785.
39. Stepanova, L., Leng, X., Parker, S. B., and Harper, J. W. (1996) *Genes Dev. 10*, 1491−1502.
40. Grammatikakis, N., Lin, J.-H., Grammatikakis, A., Tsichlis, P. N., and Cochran, B. H. (1999) *Mol. Cell. Biol. 19*, 1661−1672.
41. Shao, J., Gramatikakis, N., Scroggins, B., Uma, S., Huang, W., Chen, J.-J., Hartson, S. D., and Matts, R. L. (2001) *J. Biol. Chem. 276*, 206−214.
42. Rao, J., Lee, P., Benzeno, S., Cardozo, C., Albertus, J., Robins, D. M., and Caplan, A. J. (2001) *J. Biol. Chem. 276*, 5814−20.
43. Wang, X., Grammatikakis, N., and Hu, J. (2002) *J. Biol. Chem. 277*, 24361−7.
44. Bose, S., Weikl, T., Bugl, H., and Buchner, J. (1996) *Science 274*, 1715−7.
45. Freeman, B. C., Toft, D. O., and Morimoto, R. I. (1996) *Science 274*, 1718−20.
46. Scheibel, T., and Buchner, J. (1998) *Biochem. Pharmacol. 56*, 675−82.
47. Whitesell, L., Mimnaugh, E. G., De Costa, B., Myers, C. E., and Neckers, L. M. (1994) *Proc. Natl. Acad. Sci. U.S.A. 91*, 8324−8328.
48. Stebbins, C. E., Russo, A. A., Schneider, C., Rosen, N., Hartl, F. U., and Pavletich, N. P. (1997) *Cell 89*, 239−250.
49. Prodromou, C., Roe, S. M., O'Brien, R., Ladbury, J. E., Piper, P. W., and Pearl, L. H. (1997) *Cell 90*, 65−75.
50. Marcu, M. G., Schulte, T. W., and Neckers, L. (2000) *J. Natl. Cancer Inst. 92*, 242−8.
51. Marcu, M. G., Chadli, A., Bouhouche, I., Catelli, M., and Neckers, L. M. (2000) *J. Biol. Chem. 275*, 37181−6.
52. Soti, C., Racz, A., and Csermely, P. (2001) *J. Biol. Chem. 277*, 7066−75.
53. Hartson, S. D., Thulasiraman, V., Huang, W., Whitesell, L., and Matts, R. L. (1999) *Biochemistry 38*, 3837−3849.
54. Owen, B. A., Sullivan, W. P., Felts, S. J., and Toft, D. O. (2002) *J. Biol. Chem. 277*,7086−91.
55. Johnson, J. L., and Toft, D. O. (1995) *Mol. Endocrinol. 9*, 670−678.
56. Johnson, B. D., Schumacher, R. J., Ross, E. D., and Toft, D. O. (1998) *J. Biol. Chem. 273*, 3679−3686.
57. Sullivan, W., Stensgard, B., Caucutt, G., Bartha, B., McMahon, N., Alnemri, E. S., Litwack, G., and Toft, D. (1997) *J. Biol. Chem. 272*, 8007−8012.
58. Thulasiraman, V., and Matts, R. L. (1996) *Biochemistry 35*, 13443−13450.
59. Shao, J., Hartson, S. D., and Matts, R. L. (2002) *Biochemistry 41*, 6770−9.
60. Kreig, P. A., and Melton, D. A. (1984) *Nuc. Acids Res. 12*, 7057−7070.
61. Hartson, S. D., and Matts, R. L. (1994) *Biochemistry 33*, 8912−8920.
62. Uma, S., Matts, R. L., Guo, Y., White, S., and Chen, J.-J. (2000) *Eur. J. Biochem. 267*, 498−506.
63. Uma, S., Barret, D. J., and Matts, R. L. (1997) *Exp. Cell Res. 238*, 273−282.
64. Uma, S., Thulasiraman, V., and Matts, R. L. (1999) *Mol. Cell. Biol. 19*, 5861−5871.
65. Matts, R. L., Xu, Z., Pal, J. K., and Chen, J.-J. (1992) *J. Biol. Chem. 267*, 18160−18167.
66. Xu, Z., Pal, J. K., Thulasiraman, V., Hahn, H. P., Chen, J.-J., and Matts, R. L. (1997) *Eur. J. Biochem. 246*, 461−470.
67. Chen, G., Cao, P., and Goeddel, D. V. (2002) *Mol. Cell 9*, 401−10.
68. Brugge, J. S. (1986) *Curr. Top. Microbiol. and Immunol. 123*, 1−22.
69. Silverstein, A. M., Grammatikakis, G., Cochran, B. H., Chinkers, M., and Pratt, W. B. (1998) *J. Biol. Chem. 273*, 20090−20095.
70. Basso, A. D., Solit, D. B., Chiosis, G., Giri, B., Tsichlis, P., and Rosen, N. (2002) *J. Biol. Chem. 277*, 39858−66.
71. Hutchison, K. A., Dittmar, K. D., Czar, M. J., and Pratt, W. P. (1994) *J. Biol. Chem. 269*, 5043−5049.
72. Dittmar, K. D., Demady, D. R., Stancato, L. F., Krishna, P., and Pratt, W. B. (1997) *J. Biol. Chem. 272*, 21213-21220.
73. Morishima, Y., Murphy, P. J., Li, D. P., Sanchez, E. R., and Pratt, W. B. (2000) *J. Biol. Chem. 275*, 18054−60.
74. Kanelakis, K. C., Shewach, D. S., and Pratt, W. B. (2002) *J. Biol. Chem. 277*, 33698−703.
75. Thulasiraman, V., Yun, B. G., Uma, S., Gu, Y., Scroggins, B. T., and Matts, R. L. (2002) *Biochemistry 41*, 3742−53.
76. Stancato, L. F., Silverstein, A. M., Owens-Grillo, J. K., Chow, Y. H., Jove, R., and Pratt, W. B. (1997) *J. Biol. Chem. 272*, 4013−20.
77. Smith, D. F., Whitesell, L., Nair, S. C., Chen, S., Prapapanich, V., and Rimerman, R. A. (1995) *Mol. Cell. Biol. 15*, 6804−6812.
78. Smith, D. F., Stensgard, D. B., Welch, W. J., and Toft, D. O. (1992) *J. Biol. Chem. 267*, 1350−1356.
79. Smith, D. (1993) *Mol. Endocrinol. 7*, 1418−1429.
80. Czar, M. J., Galigniana, M. D., Silverstein, A. M., and Pratt, W. B. (1997) *Biochemistry 36*, 7776−85.
81. Kudlicki, W., Chirgwin, J., Kramer, G., and Hardesty, B. (1995) *Biochemistry 34*, 14284−7.
82. Makeyev, E. V., Kolb, V. A., and Spirin, A. S. (1996) *FEBS Lett. 378*, 166−70.
83. Hardesty, B., and Kramer, G. (2001) *Prog. Nucleic Acid Res. Mol. Biol. 66*, 41−66.
84. Schneider, C., Sepp-Lorenzino, L., Nimmesgern, E., Ouerfelli, O., Danishefsky, S., Rosen, N., and Hartl, F. U. (1996) *Proc. Natl. Acad. Sci. U.S.A. 93*, 14536−14541.
85. Schumacher, R. J., Hurst, R., Sullivan, W. P., McMahon, N. J., Toft, D. O., and Matts, R. L. (1994) *J. Biol. Chem. 269*, 9493−9499.
86. Schumacher, R. J., Hansen, W. J., Freeman, B. C., Alnemri, E., Litwack, G., and Toft, D. O. (1996) *Biochemistry 35*, 14889−14898.
87. Sala-Newby, G., Kalsheker, N., and Campbell, A. K. (1990) *Biochem. Biophys. Res. Commun. 172*, 477−82.
88. Mort-Bontemps-Soret, M., Facca, C., and Faye, G. (2002) *Mol. Genet. Genomics 267*, 447−58.
89. Gerber, M. R., Farrell, A., Deshaies, R. J., Herskowitz, I., and Morgan, D. O. (1995) *Proc. Natl. Acad. Sci. U.S.A. 92*, 4651−5.
90. Goes, F. S., and Martin, J. (2001) *Eur. J. Biochem. 268*, 2281−9.
91. Lee, P., Rao, J., Fliss, A., Yang, E., Garrett, S., and Caplan, A. J. (2002) *J. Cell Biol. 159*, 1051−9.
92. Jedlicka, P., and Panniers, R. (1991) *J. Biol. Chem. 266*, 15663−15669.

93. Russo, A. A., Jeffrey, P. D., Patten, A. K., Massague, J., and Pavletich, N. P. (1996) *Nature 382*, 325−31.
94. Moskowitz, N. K., Borao, F. J., Dardashti, O., Cohen, H. D., and Germino, F. J. (1996) *Oncol. Res. 8*, 343−52.
95. Rafie-Kolpin, M., Han, A.-P., and Chen, J.-J. (2003) *Biochemistry 42*, 6536−44.
96. Bauer, B. N., Rafie-Kolpin, M., Lu, L., Han, A., and Chen, J. J. (2001) *Biochemistry 40*, 11543−51.
97. Williams, J. C., Wierenga, R. K., and Saraste, M. (1998) *Trends Biol. Chem. 23*, 179−184.
98. Grenert, J. P., Sullivan, W. P., Fadden, P., Haystead, T. A. J., Clark, J., Mimnaugh, E., Krutzsch, H., Ochel, H.-J., Schulte, T. W., Sausville, E., Neckers, L. M., and Toft, D. O. (1997) *J. Biol. Chem. 272*, 23843−23850.
99. Panaretou, B., Prodromou, C., Roe, S. M., O'Brien, R., Ladbury, J. E., Piper, P. W., and Pearl, L. H. (1998) *EMBO J. 17*, 4829−4836.
100. Obermann, W. M. J., Sondermann, H., Russo, A. A., Pavletich, M. P., and Hartl, F. U. (1998) *J. Cell Biol. 143*, 901−910.
101. Weikl, T., Muschler, P., Richter, K., Veit, T., Reinstein, J., and Buchner, J. (2000) *J. Mol. Biol. 303*, 583−92.
102. Johnson, B. D., Chadli, A., Felts, S. J., Bouhouche, I., Catelli, M. G., and Toft, D. O. (2000) *J. Biol. Chem. 275*, 32499−507.
103. Prodromou, C., Panaretou, B., Chohan, S., Siligardi, G., O'Brien, R., Ladbury, J. E., Roe, S. M., Piper, P. W., and Pearl, L. H. (2000) *EMBO J. 19*, 4383−92.
104. Young, J. C., and Hartl, F. U. (2000) *EMBO J. 19*, 5930−40.
105. Richter, K., Muschler, P., Hainzl, O., and Buchner, J. (2001) *J. Biol. Chem. 276*, 33689−96.
106. Siligardi, G., Panaretou, B., Meyer, P., Singh, S., Woolfson, D. N., Piper, P. W., Pearl, L. H., and Prodromou, C. (2002) *J. Biol. Chem. 277*, 20151−9.
107. Sullivan, W. P., Owen, B. A., and Toft, D. O. (2002) *J. Biol. Chem. 277*, 45942−8.
108. McLaughlin, S. H., Smith, H. W., and Jackson, S. E. (2002) *J. Mol. Biol. 315*, 787−98.
109. Hernandez, M. P., Sullivan, W. P., and Toft, D. O. (2002) *J. Biol. Chem. 277*, 38294−304.
110. Langer, T., Schlatter, H., and Fasold, H. (2002) *Cell Biol. Int. 26*, 653−7.
111. Panaretou, B., Siligardi, G., Meyer, P., Maloney, A., Sullivan, J. K., Singh, S., Millson, S. H., Clarke, P. A., Naaby-Hansen, S., Stein, R., Cramer, R., Mollapour, M., Workman, P., Piper, P. W., Pearl, L. H., and Prodromou, C. (2002) *Mol. Cell 10*, 1307−18.

BI035001T